Springer

Journal of Mechanical Science and Technology 22 (2008) 1984~1992

Journal of Mechanical Science and Technology

www.springerlink.com/content/1738-494x
DOI 10.1007/s12206-008-0743-8

Blade number effect for a ducted wind turbine †

Sheng-Huan Wang and Shih-Hsiung Chen*

Department of Aeronautics and Astronautics, National Cheng Kung University, 701, No. 1, University Road, Tainan City, Taiwan

(Manuscript Received April 16, 2008; Revised June 25, 2008; Accepted July 23, 2008)

Abstract

Ducted wind turbine with multiple blades installed was believed to have a good wind power energy conversion effect. However, little information was available on how to design a good ducted wind turbine. In this paper the effects of blade number on a ducted wind turbine performance is studied. Numerical studies using CFD method to simulate the wind turbine performance were adopted. The duct is a converging-diverging nozzle with the turbine blades located at the throat. A rated output of a 1-kW turbine is adopted as the baseline design. It was found that the blade geometry, stagger angle, and number of blades have different duct blockage effects, and do affect the turbine performance (specifically the power coefficient and torque coefficient, etc.). The fewer number of blades has higher through flow speed, while the larger number of blades provides larger torque. The best power coefficient lies in between the two extremes. The appropriate number of blades is important to match the generator performance curve for optimal overall performance and efficiency.

Keywords: Wind turbine; Duct; CFD; Aerodynamics; Blockage effect; Number of blades

1. Introduction

It was realized that a multi-blade convergent-inlet and divergent-outlet ducted wind turbine design (or so called diffuser augmented wind turbine (DAWT)) does have aerodynamic advantages over traditional 3-bladed propeller type wind turbine in converting wind energy to electric power. A converged inlet duct for accelerating wind speed and thus higher dynamic pressure over the turbine blades is incorporated with a diverged tail section for adjusting the turbine exit pressure to achieve higher power output. Blade number more than 3 is frequently considered for this ducted design in order to maximize the conversion of wind energy to blade torque. However, with blade number increased the blockage effect tends to reduce the air flow entering the duct and thus sacrifice the use of wind energy. While wind turbine is designed to match the generator performance curve for optimal overall performance and efficiency, the blade shape design is critical to achieve this goal. The 3-D blade shape determination relies heavily on the inflow velocity and blade rotating speed. While the blockage effect affects the incoming wind speed, and in return the wind speed determines the blade configuration and thus the blockage, the interaction between wind, duct and blades are complicated. The precise determination of the wind speed approaching the turbine blades is critical in the design process. Design iteration is needed in order to best determine the incoming flow and thus the blade angles at all sections. The purpose of this paper is to present the design procedure for the ducted wind turbine with many turbine blades installed. The computational fluid dynamics (CFD) technique is used in the study. A rated output of a 1-kW turbine is adopted as the baseline design. In the study a predetermined ducted shape is given, while the number of blade is varying. In the paper, the process of design iteration for a given blade number and the number of blade effects on the overall per-

† This paper was presented at the 9th Asian International Conference on Fluid Machinery (AICFM9), Jeju, Korea, October 16-19, 2007.

*Corresponding author. Tel.: +886 928628298, Fax.: +886 6 2362524
E-mail address: shchen86@hotmail.com

formance are presented.

In 1919, Betz provided the theory of the wind turbine in which the maximum power coefficient is about 59%. Most researchers made efforts in the increase of the efficiency of the wind turbine. However although the horizontal axial wind turbines (HAWT) and vertical axial wind turbines (VAWT) have been improved in their designs, the efficiency seemed to barely reach about 42%. Kogan and Nissim [1] and Kogan and Seginer [2] first referred to the wind turbine with convergent entrance and divergent exit that could reduce the cut-in speed. In their experiment, while the ratio of the duct length to the minimum duct diameter was 7 to 1 and the drag coefficient of the duct was between 0.18 and 0.22, the higher efficiency was presented. After Kogan et al., Igra [3] did a series of experiments extending previous reach by adopting standard airfoil (NACA4412) as the sectional profile of the duct and putting emphasis on the change of the pressure gradient at diffuser exit. The results were shown that the pressure at the diffuser exit could be reduced by adding a few ring-shaped airfoils around it and the efficiency was raised to 52%. Duquette et al. [4] and Duquette and Visser [5] used the simulation and the experimental data comparison to study the influence of the number of blades on efficiency. They provided that the wind turbine has 44% efficiency with 12 blades. This result improved the efficiency of the multi-blades wind turbine improved upon Johnson's study [6] by about 30%. Grassmann and Bet [7] used the numerical simulation to compare the pressure distribution between the non-ducted and ducted wind turbine. The result showed that the power of a wind turbine was increased by a factor of 2.0 by means of wing structure placed at some distance around the turbine. Frankovic and Vrsalovic [8] estimated that the efficiency of the ducted wind turbine could be raised 3.5 times while the area of the inlet was 3 times of the minimum section.

While in past years, most researches have placed emphasis on how the ducted wind turbine transforms energy effectively, literature on the issue of the effect of the number of blades on the overall performance is still lacking. Thus the major purpose of this present study is to investigate the energy transformation from wind energy to mechanical energy of the ducted wind turbine with varying the number of blades and provide the blade design process under the adopted duct geometry, blade chord distribution and number of blades. The research method comprises an analysis based on the use of computational fluid dynamics (CFD) technique. A rated output of a 1-kW turbine was adopted as the baseline design to match the generator at 12 m/s wind speed and 1000 rpm rotating speed.

To investigate the influence of the number of blades on the blade entrance velocity, two types of blades were used. Torque and power coefficients were obtained according to the CFD results of the pressure distribution on the blade surface at 12m/s wind speed and various rotating speed.

2. Problem description and computational method

2.1 Physical model

An adopted wind turbine is composed of the duct, spinner, hub and blades. The duct is 1 meter in length with the convergent inlet and divergent exit. The diameter of the inlet is 1.506 meters, the exit is 2 meters and the minimum section (i.e. throat) is 1.44 meters. The throat is located 0.3 meters distance from the inlet of the duct, i.e. 30 % length of the duct. The hub and spinner with 0.2 meters diameter are in the central axis. In practice the generator will be seated in the hub.

From root to tip, the thickness, chord length, and stagger angle of the blade are various. In this study the gravity and structural load distribution is considered larger at the root than the tip, and therefore, the general airfoil NACA4420, NACA4416 and NACA4412 were adopted to produce various blade profiles. Because NACA4412 has the highest lift/drag ratio approximately at 7 degrees angle of attack, all sectional incidence angles of the blade profiles were set 7 degrees. The blade chord distribution is shown in Fig. 1. Based on these blade parameters blade profiles were illustrated (Fig. 2) and produce 3-D geometry.

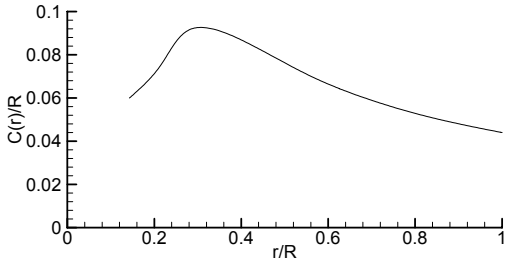

Fig. 1. The chord distribution of the wind turbine blade.

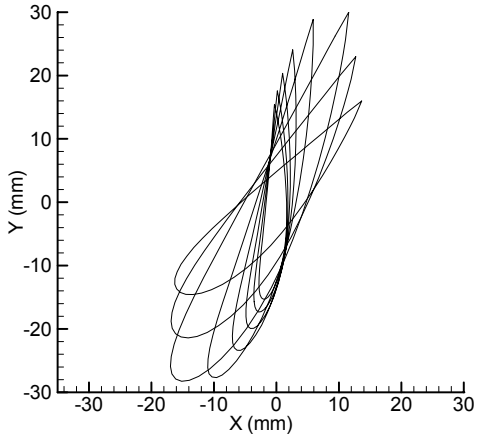

Fig. 2. Blade profile cross sections.

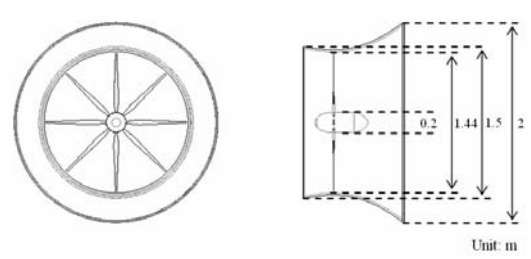

Fig. 3. The overall wind turbine.

The overall wind turbine is shown in Fig. 3. In order to achieve the maximum blade entrance velocity blades were installed at throat. The tip clearance is 20 millimeters and the diameter of the blade is 1.4 meters.

2.2 Mesh system

Unstructured meshes were constructed using the mesh generator ANSYS ICEM CFD in this study. The zonal boundary of the wind turbine flow field was divided into two parts. One is the outer flow field (Fig. 4) in which the upstream boundary of computational domain is four diameters (4×D) from the entrance of the duct; the downstream boundary is 10×D from the exit of the duct and the lateral surrounding boundary is 2×D from the side of the duct. And the other is inner flow field that is the rotating mesh surrounding the blade of wind turbine.

In general, the axial symmetrical flow field was configured in the rotor to simplify the physical problem, decrease the requirement of random-access memory and save computational time. Furthermore, since the flow field is a steady state corresponding to

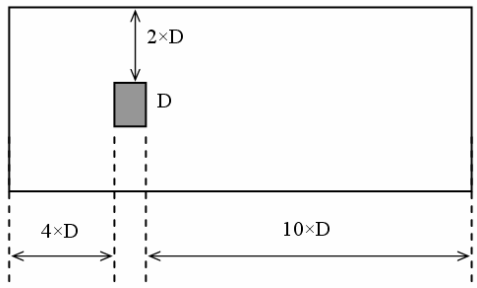

Fig. 4. Boundary of the computational outer flow field.

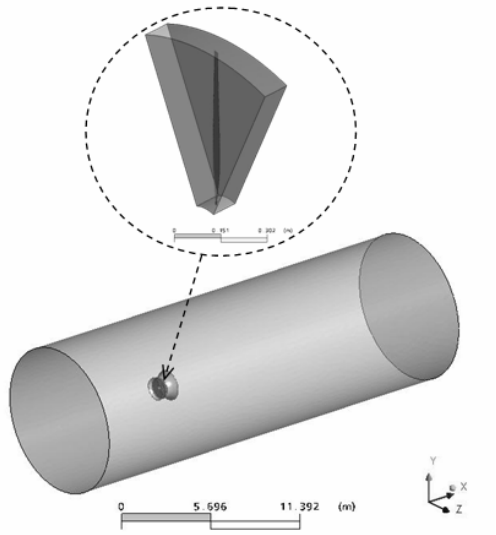

Fig. 5. The complete mesh system.

the rotor coordinate system, the single blade-centered flow passage, shown in Fig. 5, was chosen to simulate the whole rotor flow field. It has periodical variation and single flow inlet and exit.

2.3 CFD simulation

CFD analysis was made using a commercially available package, ANSYS CFX. This package has been successfully used in the flow field simulation and design for tubomachinery. The numerical method was to solve Reynolds-averaged Navier-Stokes Equations by finite volume method. The k-ε turbulent model with wall function was adopted to predict the complex turbulent flow field.

The inner flow field mesh domain was rotating, and hence, the coordinate system of the numerical simulation was fixed on the rotor coordinate system. The solution of the velocity was relative velocity.

Furthermore, the outer flow field domain was fixed on the absolute coordinate system and the solution of the velocity was absolute velocity. Thus the velocity and other parameters between the interfaces of the two domains should be done coordinate transformation to conserver mass, momentum and energy.

2.4 Boundary condition

Inlet boundary condition 12 m/s axial flow velocity was set on the inlet of the outer flow field domain. Opening boundary conditions were set on the surrounding surface and exit of the outer flow field domain. This specifies that the static pressure corresponds with 1 atmosphere pressure.

Wall boundary conditions were set on pressure and suction surfaces of the blade, and the duct and hub surfaces. This specifies that the fluid cannot flow across the boundary. For viscous flow, the no-slip condition should be satisfied i.e. the flow velocity at the wall is equal to the velocity of the wall. Periodic boundary conditions were set on the boundary surfaces in the tangential direction. The solution is identical on the pair of boundary surfaces. Stage interface conditions were set between the two domains.

3. Results and discussion

First, under the determined duct geometry and the rated wind speed, the flow field only with the duct and hub was simulated with CFD method. The velocity of the incoming wind speed certainly could be accelerated by this duct. The result of the velocity distribution is shown in Fig. 6 and the mean velocity at the throat is approximately 22.22 m/s. And then in the CFD simulation the number of blades was varied in 2, 4, 6 and 8 with two types, Blade A and Blade B. They have the same chord distribution as shown in Fig. 1 and the difference in the estimated blockage factor. According to the blade geometry parameters, as shown in Table 1 and Table 2, the blade profile cross sections were illustrated to produce the three-dimensional outline.

Performance parameters are defined as the following:

$$\text{Tip Speed Ratio: } \lambda = \frac{2\pi R\Omega / 60}{V_\infty}$$

$$\text{Augmentative Velocity Ratio: } \varepsilon = \frac{V_B}{V_\infty}$$

Table 1. The parameters of Blade A.

Airfoil	r/R	Flow Angle φ (deg.)	Incidence Angle α (deg.)	Stagger Angle θ (deg.)
NACA 4420	0.143	51.85	7	45.15
NACA 4416	0.286	32.48	7	64.52
NACA 4412	0.429	22.99	7	74.01
NACA 4412	0.714	14.28	7	82.72
NACA 4412	1	10.31	7	86.69

Table 2. The parameters of Blade B.

Airfoil	r/R	Flow Angle φ (deg.)	Incidence Angle α (deg.)	Stagger Angle θ (deg.)
NACA 4420	0.143	59.49	7	37.51
NACA 4416	0.286	40.31	7	56.69
NACA 4412	0.429	29.49	7	67.51
NACA 4412	0.714	18.75	7	78.25
NACA 4412	1	13.63	7	83.37

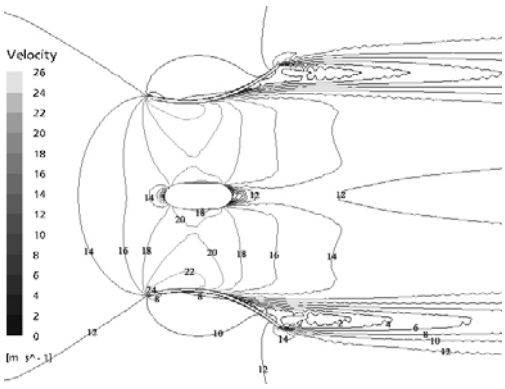

Fig. 6. Velocity distribution at $V_\infty = 12$ m/s.

$$\text{Power Coefficient: } C_P = \frac{P}{\frac{1}{2}\rho\pi R^2 V_\infty^3}$$

$$\text{Torque Coefficient: } C_T = \frac{T}{\frac{1}{2}\rho\pi R^3 V_\infty^2}$$

3.1 The wind turbine with 2 blades

Fig. 7 shows the power coefficient of the turbine with 2 blades relative to the tip speed ratio. The maximum power coefficient of Blade A and Blade B are presented at $\lambda = 8.55$ and $\lambda = 7.33$. At 12 m/s wind speed, their corresponding rotating speeds are 1400 and 1200 rpm. These results obviously diverge from the design point (i.e. $\lambda = 6.11$).

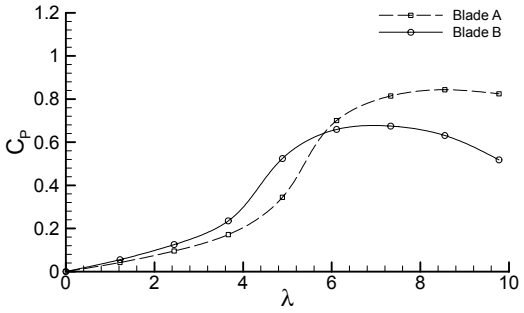

Fig. 7. Power coefficient of the turbine with 2 blades relative to the tip speed ratio.

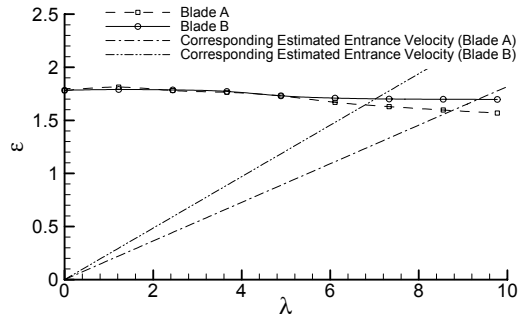

Fig. 8. Augmentative velocity ratio of the turbine with 2 blades relative to the tip speed ratio.

In Fig. 8, the reason is explained that the blade entrance velocity decreased slightly with the increasing λ and the blockage effect of these two types with 2 blades was lighter, and therefore at $\lambda = 6.11$, the simulated blade entrance velocity is higher than the estimated. As a result the incidence angle is higher and the maximum C_P is appeared at high λ. The decreasing blade entrance velocity and the raising rotating speed with increasing λ causes the incidence angle gradually reduced to about 7 degrees. And further, a little differences of the blade entrance velocity between Blade A and Blade B are not presented until the tip speed ratios reach $\lambda = 6.11$, that is to say, the blockage effect of the blade stagger angle became noticeable at high λ.

Fig. 9 shows the torque coefficient of the turbine with 2 blades relative to the tip speed ratio. While the tip speed ratio is in lower region the torque coefficient of Blade B is higher than Blade A. While λ reaches approximately to 5.4, the incidence angle of Blade B is reduced to 10 degrees with corresponding maximum C_T but the incidence angle of Blade A is not reduced to 10 until $\lambda = 6.2$. In the high λ region all the incidence angles are lower than 10 degrees and

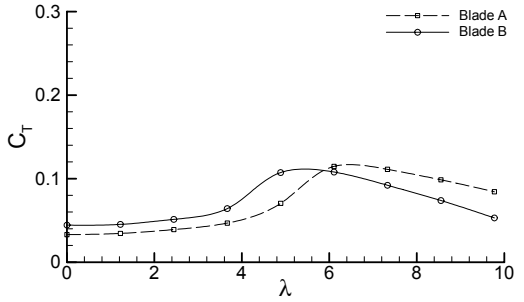

Fig. 9. Torque coefficient of the turbine with 2 blades relative to the tip speed ratio.

Blade A is larger than Blade B. Thus the C_T of Blade A is larger than Blade B. Briefly, for the ducted wind turbine with 2 blades the blockage effect is small and causes the blade entrance velocity reduced slightly. So the main effect on the performance is the blade stagger angle and this consequence is similar to the 3-bladed propeller type wind turbine.

3.2 The wind turbine with 4 blades

Fig. 10 shows the power coefficient of the turbine with 4 blades relative to the tip speed ratio. The maximum power coefficient of Blade A and Blade B are presented at $\lambda = 6.2$. At 12 m/s wind speed their corresponding rotating speeds are about 1015 rpm, and that the C_P of Blade B is larger than Blade A on account of the higher estimated blade entrance velocity due to the small blockage in the duct. Moreover, the more mass flow rate through the duct brought about higher flow velocity and led to the more power output of the wind turbine. That is proved again in Fig. 11. It can be seen that the entrance velocity of Blade B is larger than Blade A at $\lambda = 6.11$. Furthermore, in the low λ region the blade entrance velocity of Blade A is similar to Blade B. Overall while λ is over 4.8 the blade entrance velocity of the differences between Blade A and Blade B become evident. In Fig. 12, the torque coefficient of the turbine with 4 blades relative to the tip speed ratio is shown. After $\lambda = 4.8$, the torque coefficient of Blade B begins reducing with the increasing λ, but Blade A does not until $\lambda = 6$.

3.3 The wind turbine with 6 blades

Fig. 13 shows the power coefficient of the turbine with 6 blades relative to the tip speed ratio. The maximum power coefficient of Blade A and Blade B

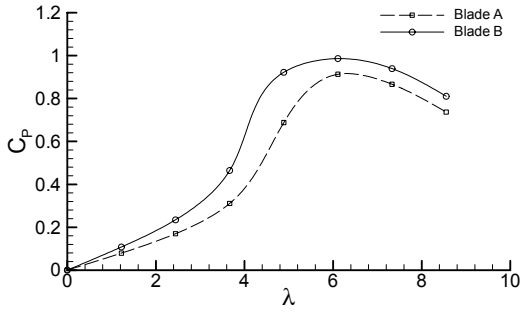

Fig. 10. Power coefficient of the turbine with 4 blades relative to the tip speed ratio.

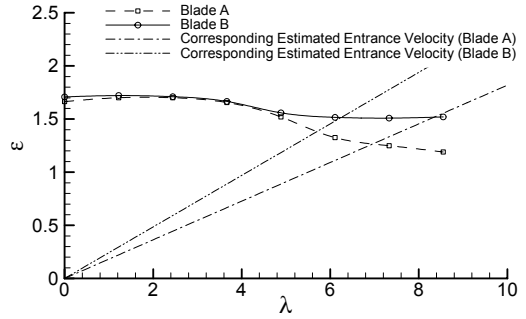

Fig. 11. Augmentative velocity ratio of the turbine with 4 blades relative to the tip speed ratio.

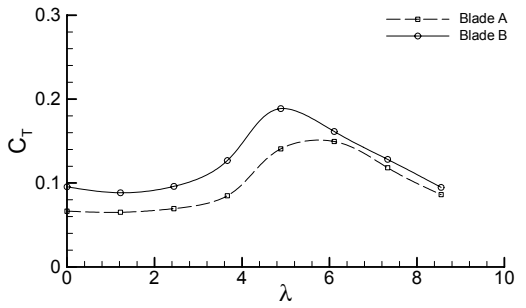

Fig. 12. Torque coefficient of the turbine with 4 blades relative to the tip speed ratio.

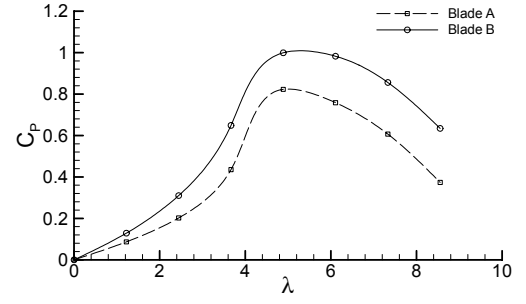

Fig. 13. Power coefficient of the turbine with 6 blades relative to the tip speed ratio.

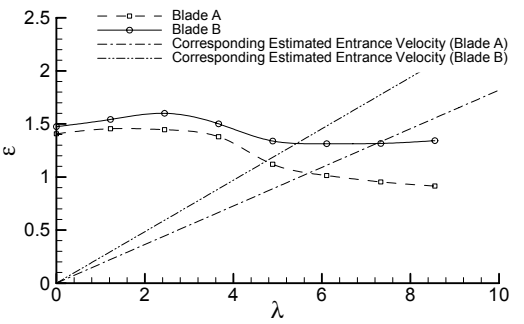

Fig. 14. Augmentative velocity ratio of the turbine with 6 blades relative to the tip speed ratio.

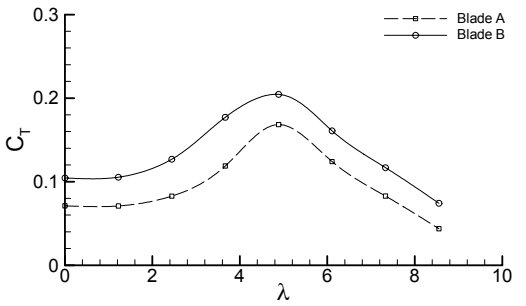

Fig. 15. Torque coefficient of the turbine with 6 blades relative to the tip speed ratio.

are presented at $\lambda = 5$. The reason for these results, obviously diverging from the design point, is the increasing blockage effect of using 6 blades. Moreover, one can see the simulated entrance velocity is lower than the estimated in Fig. 14. In the entire λ region the power coefficient of Blade B is larger than Blade A, and proving that the blockage effect on Blade A with large stagger angle is in evidence. Thus the blade entrance velocity of Blade A drops more. In Fig. 15 the maximum C_T of Blade A and Blade B have appeared at $\lambda = 4.8$ in accordance with the flow angle from CFD results and from the stagger angles of the two type of Blades. The incidence angle at $\lambda = 4.8$ is about 10 degrees.

3.4 The wind turbine with 8 blades

Fig. 16 shows the power coefficient of the turbine with 8 blades relative to the tip speed ratio. The maximum power coefficient of Blade A and Blade B are presented at $\lambda = 4.8$. The reason that these results obviously diverge from the design point is the blockage effect of using 8 blades is more significant than 6 blades. As noted above, the simulated entrance velocity is lower than the estimated at $\lambda = 6.11$ as

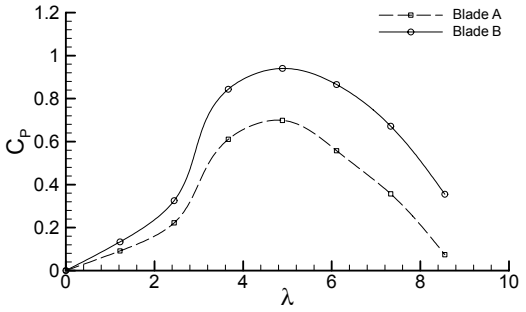

Fig. 16. Power coefficient of the turbine with 8 blades relative to the tip speed ratio.

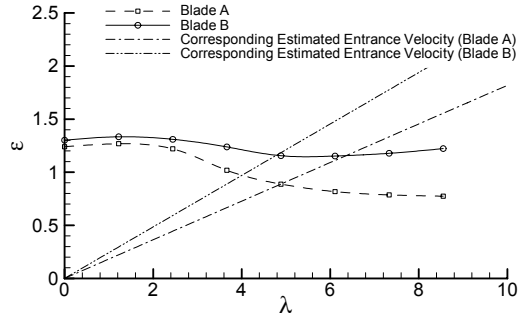

Fig. 17. Augmentative velocity ratio of the turbine with 8 blades relative to the tip speed ratio.

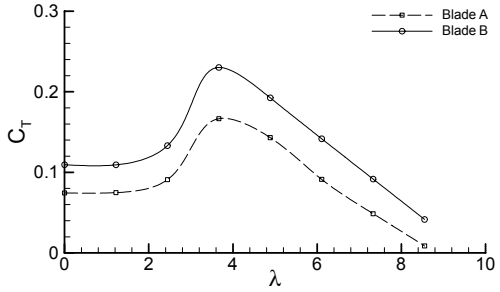

Fig. 18. Torque coefficient of the turbine with 8 blades relative to the tip speed ratio.

shown in Fig. 17. In the high λ region, the entrance velocity of Blade A decreases more with the increasing λ. Besides, the blade entranced velocity does not drop obviously until $\lambda = 2.5$. In Fig. 18 indicates the maximum torque coefficient of Blade A and Blade B are presented at $\lambda = 3.7$.

3.5 Various blade numbers for blade A

It was estimated the lower blade entrance velocity in Blade A with larger stagger angle which caused more blockage effect on incoming flow.

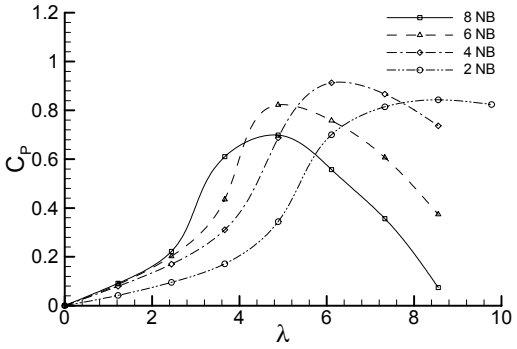

Fig. 19. Power coefficient of the turbine using Blade A with various number of blades relative to the tip speed ratio.

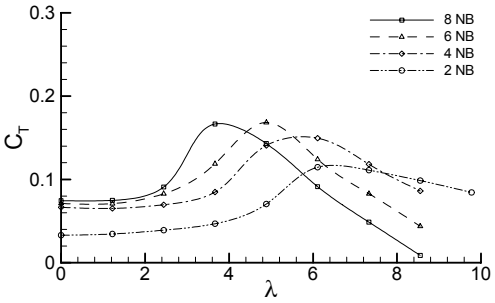

Fig. 20. Torque coefficient of the turbine using Blade A with various number of blades relative to the tip speed ratio.

Thus reducing the number of blades could be beneficial for wind to flow into the duct and increase the blade entrance velocity. The power coefficient of the ducted wind turbine using Blade A is presented in Fig. 19. One can find that when the turbine uses 4 blades the larger power coefficient can be achieved. In addition, with the reducing number of blades the maximum power coefficient appears at higher λ. Although using 2 blades could reduce the blockage effect and raise the blade entrance velocity, it was deficient in blade area to absorb wind energy. For this reason the maximum coefficient is lower than using 4 blades.

Fig. 20 shows the torque coefficient of Blade A with the various number of blades relative to the tip speed ratio. One can see that the maximum torque coefficient of using 6 and 8 blades are larger than others but their corresponding tip speed ratios are lower than the design point ($\lambda = 6.11$). The increasing number of blades caused the blade entrance velocity to be reduced and lower than the estimated at design point. Furthermore, the corresponding torque coefficient at $\lambda = 0$ (i.e. the available driving mo-

ment for the wind turbine) drops with various number of blades. The differences among using 8, 6 and 4 blades are in 10% range, but the value of using 2 blades is lower 50% than using 4 blades. More specifically, the increasing number of blades can raise the torque coefficient and then reduce the cut-in speed of the wind turbine.

3.6 Various blade numbers for blade B

It was estimated the higher blade entrance velocity in Blade B with smaller stagger angle which caused less blockage effect on incoming flow. Compared with Blade A, it could permit to using more blades which provide more starting torque. The power coefficient of the ducted wind turbine using Blade B is presented in Fig. 21. One can see that larger power coefficient in the turbine can be achieved by using 6 blades. And, with the reducing number of blades the maximum power coefficient is appeared at higher λ. Although using 2 blades could reduce the blockage effect and raise the blade entrance velocity, it was deficient in blade area to absorb wind energy as above. So the maximum coefficient was evidently the lowest value among the various number of blades.

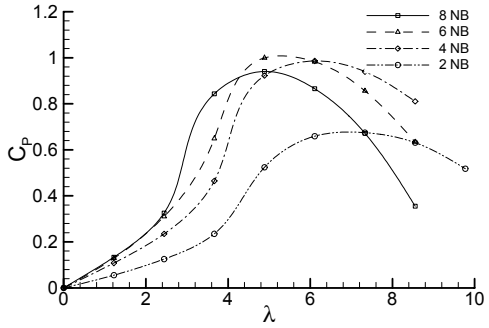

Fig. 21. Power coefficient of the turbine using Blade B with various number of blades relative to the tip speed ratio.

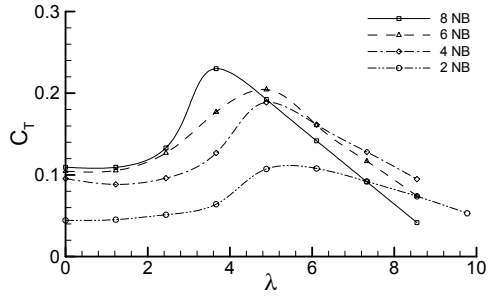

Fig. 22. Torque coefficient of the turbine using Blade B with various number of blades relative to the tip speed ratio.

Fig. 22 shows the torque coefficient of Blade B with various number of blades relative to the tip speed ratio. The maximum torque coefficient of using 8 blades is larger than others but their corresponding tip speed ratio is much lower than $\lambda = 6.11$. Furthermore, the corresponding torque coefficient at $\lambda = 0$ drops with various number of blades. The differences among using 8, 6 and 4 blades are in 10% range, but the value of using 2 blades is lower 50% than using 4 blades. This result is consistent with Blade A.

From the comparison between Fig. 20 and Fig. 22, one can find that the starting torque of Blade B is larger than Blade A as using the same number of blades. That is to say, the wind turbine with Blade B is easier to start, with the help of higher blade entrance velocity and higher tangential force produced due to smaller stagger angle.

4. Conclusions

The number of blade effect on a ducted wind turbine was studied with the use of CFD technique. On the whole, the increasing number of blades effectively creates the higher starting torque, reduces cut-in speed and provides the sufficient blade areas to transfer wind energy. But higher number of blades leads to more blockage and lower blade entrance velocity. Eventually the power coefficient will be reduced. For this reason the appropriate number of blades and optimizing blade design are able to match the generator performance curve for optimal overall performance and efficiency.

Acknowledgment

This study was supported by Jetpro Technology, Inc. Their financial and technical supports are acknowledged.

Nomenclature

C_P : Power coefficient
C_T : Torque coefficient
P : Power (W)
T : Torque (N-m)
N_B : Number of blades
B : Blockage factor
$C(r)$: Local chord length (m)
D : Duct exit diameter (m)
R : Turbine radius (m)
r : Local turbine radius (m)

V_B : Blade entrance velocity (m/s)
V_∞ : Wind speed (m/s)
Ω : Rotating speed (rpm)
ρ : Wind density (kg/m^3)
λ : Tip speed ratio
φ : Flow angle (deg.)
α : Incidence angle (deg.)
θ : Stagger angle (deg.)
ε : Augmentative velocity ratio

References

[1] A. Kogan and E. Nissim, Shrouded aerogenerator design study, two-dimensional shroud performance, *Bulletin of the Research Council of Israel*, 11 (1962) 67-88.

[2] A. Kogan and A. Seginer, Shrouded aerogenerator design study Ⅱ, axisymmetircal shroud performance, Proceedings of the Fifth Israel Annual Conference on Aviation and Astronautics, Israel, (1963).

[3] O. Igra, Shrouds for aerogenerators, *AIAA Journal*, Oct. (1976) 1481-1483.

[4] M. M. Duquette, C. J. Humiston and K. D. Visser, Small wind turbine research at clarkson university, *AWEA Wind Power 2002*, Portland Oregon, Jun. 4-7 (2002).

[5] M. M. Duquette and K. D. Visser, Numerical implications of solidity and blade number on rotor performance of horizontal axis wind turbines, *Journal of Solar Energy Engineering*, Nov. (2003) 42-432.

[6] G. L. Johnson, Wind Energy Systems, Prentice Hall, Englewood Cliffs, New Jersey, (1985).

[7] F. Grassmann and H. Bet, Upgrading conventional wind turbines, *Renewable Energy*, 28 (2003) 71-78.

[8] B. Frankovic and I. Vrsalovic, New high profitable wind turbines, *Renewable Energy*, 24 (2001) 491-499.